UNLIMITED DISTRIBUTION

51517

National Defence
Research and Development Branch

Défense nationale
Bureau de recherche et développement

VARIABILITY OF SHIP NOISE MEASUREMENTS

Neil Sponagle

June 1988

Approved by L.J. Leggat Director/Technology Division

DISTRIBUTION APPROVED BY

D/TD

TECHNICAL MEMORANDUM 88/210

Defence Research Establishment Atlantic

Centre de Recherches pour la Défense Atlantique

Canada

Abstract

Ship noise measurements are subject to relatively large variations that should be considered when these data are used. For modern naval ships operating at high speeds, propeller cavitation is the dominant source of radiated noise. This paper examines the variability of the broadband component of propeller cavitation noise based on statistical analysis of repeated measurements for several ships and propellers and on a conceptual model of the measurement process. Confidence intervals are determined for measured noise spectra and correlations are sought between the variability and certain important parameters. To explain these results, a number of phenomena are discussed that affect either the sound transmission properties of the water, the measurement procedure, or the acoustic source strength of propeller cavitation.

Résumé

Les mesures du bruit associé aux navires peuvent présenter des variations relativement importantes dont il faut tenir compte lorsque l'on utilise ces données. En ce qui concerne les navires de guerre modernes très rapides, la cavitation due aux hélices constitue la principale source de bruit rayonné. Dans le présent rapport, on examine la variabilité de la composante à large bande du bruit associé à la cavitation due aux hélices on se fondant sur l'analyse statistique de mesures répétées avec plusieurs navires et hélices ainsi que sur un modèle théorique de la méthode de mesure. On détermine des intervalles de confiance pour des spectres de bruit mesurés et on cherche des corrélations entre la variabilité et certains paramètres importants. Pour expliquer les résultats, on examine un certain nombre de phénomènes qui influent sur les caractéristiques de transmission acoustique de l'eau, sur la méthode de mesure ou encore sur la force de la source de bruit associé à la cavitation.

Contents

Notation

A_r	reflection coefficient
B_e	resolution bandwidth
$b_0, b_1, \ldots, b_9$	regression coefficients
c	speed of sound
f	frequency
f_m	measured frequency
f_s	source frequency
g	gravitational acceleration
h	water depth
L	equivalent source pressure level
$\overline{L}$	sample mean of L
$\hat{L}$	regression value of L
m	number of data points
n	propeller revolution rate
P	acoustic pressure
P_0	reference acoustic pressure (taken to be 1 micro-pascal)
P_c	range corrected acoustic pressure
P_m	measured acoustic pressure
P_n	acoustic pressure due to noise
P_s	free-field acoustic source pressure
R^2	coefficient of multiple determination
r	distance from ship to measuring hydrophone
r_0	reference distance (take to be 1 metre)
r_d	length of direct sound path
r_m	measured to distance between sound source and receiver
r_r	length of reflected sound path
S	spectral density
S_e	estimated spectral density
S_s	spectral density of P_s
s^2	sample variance of L
$\hat{s}^2$	sample variance of L about the regression value
T	measurement time
t	time
$t_{\gamma/2}$	value of the student t probability distribution
u	ship speed
x	position along ship track
y	distance to closest point of approach of ship
z_m	depth of measurement hydrophone
z_s	depth of acoustic source
$z_{\gamma/2}$	value of the standard normal probability distribution
α	logarithmic attenuation coefficient
α_e	attenuation coefficient
β	angle of incidence

θ	angle
μ	mean of L
σ^2	variance of L
σ_s	sea surface roughness
σ_{S_e}	variance of S_e
σ_{r_m}	variance of r_m
σ_{P_m}	variance of P_m
τ_d	retarded time for direct path
τ_r	retarded time for reflected path
$\chi^2_{\gamma/2}, \chi^2_{1-\gamma/2}$	values of the chi squared probability distribution
ω	angular frequency

1 Introduction

Estimates of the noise radiated by naval vessels into the surrounding water are required to evaluate both the performance of onboard acoustic sensors and the probability of detection by other vessels. This information usually is obtained at special noise ranges, where the radiated noise may be measured with the vessel operating under controlled conditions. Such measurements often are required during the initial trials of a new vessel to enforce the builder's contractual obligations. Also, measurements may be performed at regular intervals throughout the life of a vessel to evaluate the need for maintenance, as well as before and after modifications such as a change of propeller.

Radiated noise spectra from sister ships, at the same nominal conditions, may be quite different. Even the same ship may produce noise with different spectral characteristics at different times. This suggests that ship noise measurements may include relatively large random variations. If this is true, then any comparison of ship noise measurements either with other data of the same type or with the results of a prediction method (such as scale-model tests or computer models) should differentiate between variations that are certain to be significant and those that may be due to unavoidable randomness of the data. Alternatively, if causes can be found that explain a portion of this variability, it may be possible to reduce the variability by controlling these factors or by correcting for their effects.

Figure 1 shows a set of typical radiated noise spectra for modern naval surface ships. At low ship speeds, groups of narrow bandwidth lines, caused by various pieces of rotating machinery in the ship, dominate the spectrum. At higher speeds propeller cavitation usually becomes the dominant noise source. This sound has two distinctive components. Harmonics of the propeller blade passage frequency are created by periodic variations of the cavitation as the propeller turns. Also, broadband sound is produced with maximum output at several hundred Hertz. It is this broadband component of ship noise that is considered here.

The goals of this paper are to provide a quantitative understanding of the variability in the broadband component of full-scale propeller cavitation noise measurements, identify (to the extent possible) reasons for the variability, and provide a framework for drawing conclusions from these data. The presentation will proceed as follows. First, Section 2 examines the statistical behavior of the variability based on analysis of some currently available Canadian naval ship data. Then, Sections 3 and 4 examine a number of phenomena which affect ship noise measurements. Finally, Sections 5 and 6 make conclusions and recommendations for good noise measurement practice.

2 Data Analysis

Throughout this paper the term *ship noise variability* refers to differences among radiated ship noise spectra which cannot be directly attributed to some *measurable* cause. This definition means that any quantitative measure of the variability will depend upon how well the experimental conditions are known. A number of phenomena are discussed later in this paper which affect ship noise measurements, but which are not typically monitored, and so are considered to contribute to the noise variability. On the other hand, if it becomes practical to monitor and correct for these phenomena, then the variability would be reduced.

A collection of ship noise spectra was analysed to estimate the variability. All of the data

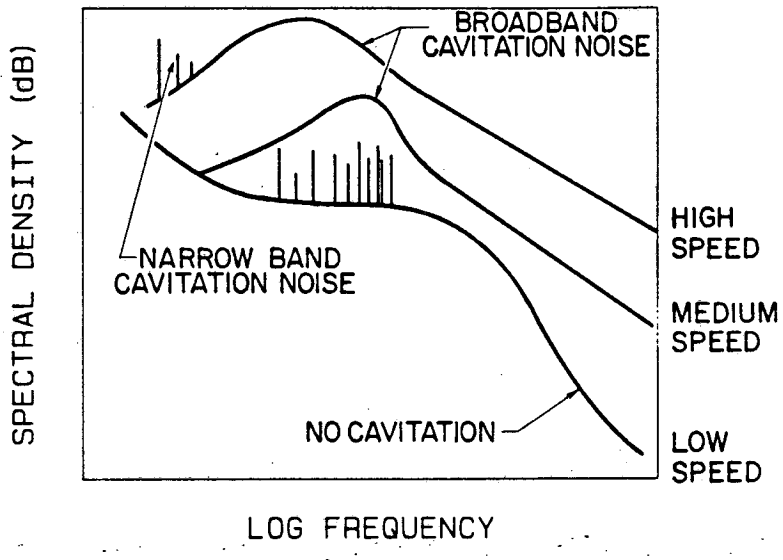

Figure 1: Typical radiated ship noise spectra at different speeds

were measured with a single omni-directional hydrophone and are presented as *equivalent source pressure levels* L defined as

$$L = 10 \log \left(\frac{1}{P_0^2 \, r_0^2 \, B_e \, T} \int_0^T r^2(t) P^2(t, f, B_e) dt \right). \tag{1}$$

Here $P(t, f, B_e)$ is the acoustic pressure measured at time t in a frequency band of width B_e centered at frequency f. The measurement is averaged over a time period of length T and the pressure is range corrected from the actual time varying range $r(t)$ to a reference range r_0 by assuming spherical spreading. The reference range is chosen to be one metre. No corrections are made for any propagation conditions that differ from spherical spreading. The values of L are expressed in terms of decibels relative to a reference pressure P_0 of one micro-pascal.

The quantity L is considered to be a random variable with statistical properties that are functions only of frequency and propeller revolution rate n. With these assumptions, the behavior of L is described by $\Pr(L \mid n, f)$, the conditional probability density for given values of frequency and propeller revolution rate n. The probability of measuring L to be between L_1 and L_2, with f and n fixed, is

$$\int_{L_1}^{L_2} \Pr(L \mid n, f) \, dL. \tag{2}$$

The mean of L is

$$\mu(n, f) = \int_{-\infty}^{\infty} L \Pr(L \mid n, f) \, dL \tag{3}$$

and the variance of L is

$$\sigma^2(n, f) = \int_{-\infty}^{\infty} (L - \mu)^2 \Pr(L \mid n, f) \, dL. \tag{4}$$

Of these, the variance is of most interest here because it is a measure of the variability of the data.

The probability density is estimated below from experimental data. From this, the confidence intervals associated with single measurements and with the mean of several measurements are deduced. Then, the data are examined for statistically significant correlations between the variability and other variables.

2.1 Analysis Procedure

2.1.1 Classical Estimation Theory

Many random processes are described by the *normal probability distribution.* If this is true for ship noise spectra (and later it will be shown to be), classical estimation theory can be used in the analysis of these data.

The analysis, as described in Reference [1], requires estimates of the mean and variance of the distribution which can be obtained from repeated measurements of L with fixed n and f. If there are m repeated measurements, the *true mean* μ is estimated by the *sample mean* $\overline{L}$, defined as

$$\overline{L} = \frac{1}{m}\sum_{i=1}^{m} L_i. \tag{5}$$

Similarly, the *true variance* σ^2 is estimated by the *sample variance* s^2, defined as

$$s^2 = \frac{1}{m-1}\sum_{i=1}^{m}\left(L_i - \overline{L}\right)^2. \tag{6}$$

Based on these quantities, the $(1-\gamma)100$ percent confidence interval for the mean μ is

$$\overline{L} - \frac{t_{\gamma/2}}{\sqrt{m}}s < \mu < \overline{L} + \frac{t_{\gamma/2}}{\sqrt{m}}s \tag{7}$$

where $t_{\gamma/2}$ is the value of the student t probability distribution, with $m-1$ degrees of freedom, which encloses an area of $1-\gamma/2$. The values of $t_{\gamma/2}/\sqrt{m}$ necessary to calculate the 95 percent confidence intervals for m from 2 to 10 are given in Table 1. As an example of their use, the 95 percent confidence interval for a sample mean calculated from five data points is $\overline{L} \pm 1.24s$. This should be interpreted as saying that, if the set of five measurements was repeated 100 times to give 100 different values of $\overline{L}$ and s, then the intervals $\overline{L} \pm 1.24s$ will contain the true mean μ at least 95 times out of the 100.

Part of the width of the above confidence interval for the mean is not associated with uncertainty in the data but with uncertainty in the estimate of the variance. The $(1-\gamma)100$ percent confidence interval for the variance σ is

$$\frac{(m-1)}{\chi^2_{\gamma/2}}s^2 < \sigma^2 < \frac{(m-1)}{\chi^2_{1-\gamma/2}}s^2 \tag{8}$$

where $\chi^2_{\gamma/2}$ and $\chi^2_{1-\gamma/2}$ are the values of the chi-square probability distribution, with $m-1$ degrees of freedom, which enclose areas of $\gamma/2$ and $1-\gamma/2$, respectively. The constants needed to calculate the 95 percent confidence intervals for m from 2 to 10 are given in Table 1. The

m	$t_{0.025}/\sqrt{m}$	$(m-1)/\chi^2_{0.025}$	$(m-1)/\chi^2_{0.975}$
2	8.98	0.20	1018.33
3	2.48	0.27	39.53
4	1.59	0.32	13.89
5	1.24	0.36	8.26
6	1.05	0.39	6.02
7	0.92	0.42	4.85
8	0.84	0.44	4.14
9	0.77	0.46	3.67
10	0.72	0.47	3.33

Table 1: Constants for 95 Percent Confidence Interval Calculation

uncertainty of the variance is very dependent upon the number of data values used to compute the estimate and can be very large for small numbers. The quantity of data available for this study (typically between two and six data points at each combination of frequency and propeller rotation rate) was not sufficient to provide acceptable accuracy using these methods alone.

If the variance of the distribution is known a priori or can be estimated by some other means, then the $(1-\gamma)100$ percent confidence interval for the mean μ is

$$\overline{L} - \frac{z_{\gamma/2}}{\sqrt{m}}\sigma < \mu < \overline{L} + \frac{z_{\gamma/2}}{\sqrt{m}}\sigma \tag{9}$$

where $z_{\gamma/2}$ is the value of the standard normal probability distribution which encloses an area of $1-\gamma/2$. The values of $z_{\gamma/2}$ are 0.67, 1.96 and 2.57 respectively for the 50, 95 and 99 percent confidence intervals. For large m, the student t distribution asymptotically approaches the normal distribution, and so Equations 7 and 9 give nearly the same confidence intervals. For small m, Equation 9 gives better results and should be used if σ can be estimated with negligible error. Regression theory provides a method to obtain this improved estimate of the variance.

2.1.2 Regression Theory

In Section 2.1.1 there was assumed to be no correlation between the statistical properties of L at different values of the independent variables, but from the physics of broadband cavitation noise, the mean equivalent source pressure level should be a *smooth* function of n and f.[1] The use of regression analysis allows this property to be exploited. In doing so an assumption must be made about the best regression model to use and the results depend to some extent on this choice. In rough terms this amounts to making an assumption about how smooth $\mu(n,f)$ is thought to be. The regression analysis methods used below are described in detail in Reference [2].

Figures 1 and 2 show the typical dependence of ship noise on frequency and ship speed [3]. The data used in this study also follow these trends and similar plots showed that, in the frequency range above the spectral peak, the noise level is a smooth enough function of n and

[1]The assumption of smoothness excludes any consideration of tonal noise components.

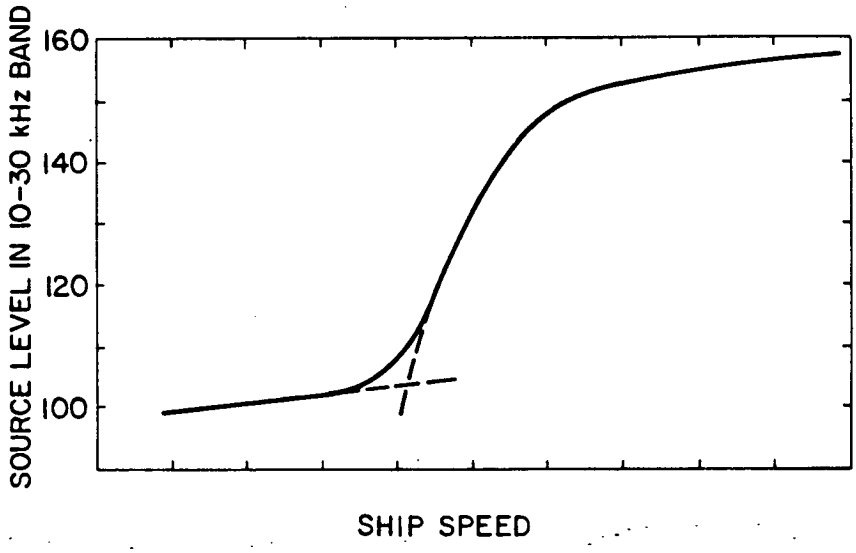

Figure 2: Typical variation of spectrum level with ship speed (figure reprinted from Reference [3])

f that the following two-variable third-order polynomial regression model can be used:

$$\hat{L}(n,f) = b_0 + b_1 n + b_2 n^2 + b_3 n^3 + b_4 f + b_5 f^2 + b_6 f^3 + b_7 nf + b_8 n^2 f + b_9 n f^2. \qquad (10)$$

The regression coefficients $b_0, b_1, \ldots, b_9$ are determined from a set of m data points (L_i, n_i, f_i) using the procedure in Appendix A. The limitation to frequencies above the peak in the noise spectrum is not intrinsic, and may be lifted by using either a higher order regression model or this model in restricted frequency ranges near the spectral peak and below it.

For the regression analysis the values L_i were in decibels and f was expressed in terms of octave band numbers (i.e. proportional to $\log(f)$). This combination tended to smooth out the rapid variations and allowed the use of a low order regression model.

A parameter called the *coefficient of multiple determination* R^2 is a measure of the adequacy of the regression model. (Its square root R is called the *multiple correlation coefficient.*) It is defined as

$$R^2 = \frac{\sum \left(\hat{L}(n_i, f_i) - \overline{L}'\right)^2}{\sum \left(L_i - \overline{L}'\right)^2} \qquad (11)$$

and has the value one for an exact fit and zero for no fit.[2] Here $\overline{L}'$ is the mean of all m data points, not just those with fixed n and f as in Section 2.1.1. A minimum of ten data points are required to define the coefficients in the regression model. If only ten points are used, the regression model will fit the data points exactly and $R^2 = 1$. As the number of data points is increased above ten the value of R^2 will drop and will eventually reach some stable value.

[2]A formula which is equivalent, but more efficient for computation, is given in Appendix A.

If the regression model is adequate and m is much larger than ten, then $\hat{L}$ is an unbiased estimator of μ with much smaller confidence intervals than those found in Section 2.1.1. (The calculation of the confidence interval for this type of regression model is quite complex and will not be discussed here. Interested readers should consult Section 2.6 of Reference [2].) Alternatively, if the regression model is not adequate for some values of n or f, then $\hat{L}$ is a biased estimator. The adequacy of the regression model is determined from examination of the residuals and the value of R^2, as discussed in Chapter 3 of Reference [2].

Information about the distribution of measurements around the regression value is found from examination of the ***residuals*** which are defined as

$$L_i - \hat{L}(n_i, f_i). \tag{12}$$

The variance about the regression value is given by

$$\hat{s}^2 = \frac{1}{m-10} \sum_{i=1}^{m} \left(L_i - \hat{L}(n_i, f_i) \right)^2. \tag{13}$$

2.2 Data and Results

The analysis procedure described in Section 2.1.2 was applied to actual ship noise data. The results are limited to frequencies above the peak in the cavitation noise spectrum where the regression model is adequate. Also, since broadband propeller cavitation noise was of interest, data were considered only at ship speeds where propeller cavitation was the dominant noise source and data in frequency bands with strong tonal components were dropped.

Two sets of results were calculated. First, the analysis was applied to *single data sets* which are consistent sets of noise spectra, measured within a period of a few days, with all parameters constant except propeller revolution rate. This provided information about the short term variability of ship noise as would be encountered during a typical ship noise trial. Second, *combined data sets* were formed from several single data sets for the same ship and propeller, but measured at different times over a period of several years. Analysis of these provided a measure of the long term variability which is most relevant when comparing data from several ship trials.

The data were selected from past ship noise reports produced by one of the Canadian noise ranges and are summarized in Table 2. Six combined data sets were considered, drawn from noise measurements of three ships each with several different propeller geometries. For each, the propeller cavitation was known from full-scale trials and model tests.

2.2.1 Probability Distributions

The following procedure was used to estimate the probability density function for both the single and combined data sets.

1. For each of the data sets with at least 30 points:
   (a) apply the regression model,
   (b) calculate the quantity $\hat{s}^2$, and then
   (c) estimate the probability distribution of the residuals.

ship	propeller	data set	m	Single Data Sets		Combined Data Sets	
				R^2	$\hat{s}^2$	R^2	$\hat{s}^2$
A	1	a	76	0.973	5.09	0.955	9.98
		b	10				
		c	42	0.935	5.01		
		d	86	0.983	6.28		
	2	a	60	0.982	4.00	0.937	13.84
		b	51	0.977	6.20		
B	1	a	72	0.970	5.46	0.932	9.68
		b	36	0.984	2.11		
		c	36	0.950	7.31		
	2	a	48	0.953	8.22	0.956	11.36
		b	72	0.977	3.98		
C	1	a	78	0.947	9.48	0.950	9.38
		b	12				
		c	24				
	2	a	66	0.958	7.88	0.936	11.73
		b	12				
		c	12				
average					5.92		10.99

Table 2: Summary of Data and Results

2. Form a composite probability distribution by combining the probability distributions found for each of the data sets and estimate the overall variance from the average of the separate values of $\hat{s}^2$.

This procedure is valid only if both the probability density and variance are independent of n and f. This was found to be true, as discussed in Section 2.2.2.

The coefficients of multiple determination R^2 and the estimates of variance $\hat{s}^2$ are shown in Table 2. The smallest value of R^2 is 0.932 which indicates that the regression model is adequate for these data.

For the single data sets, the average variance was 5.92 (equivalent to a standard deviation of 2.43 dB) and the composite residual probability distribution is shown in Figure 3. The normal probability distribution with zero mean and variance of 5.92 also is shown. The measured distribution is well approximated by the normal distribution especially toward the tails where 95 percent confidence limits are located.

The estimated variance for the combined data sets was 10.99. The composite probability distribution is shown in Figure 4 along with the normal distribution with zero mean and 10.99 variance. Again the normal distribution adequately describes the measured distribution.

These normal distributions were used to define confidence intervals for ship noise measurements. The values for the 50, 95, and 99 percent intervals for *single* measurements are shown in Table 3 as given by Equation 9 with $m = 1$ and $\sigma = \hat{s}$.

The variance of the combined data sets was greater than that of the single data sets. This

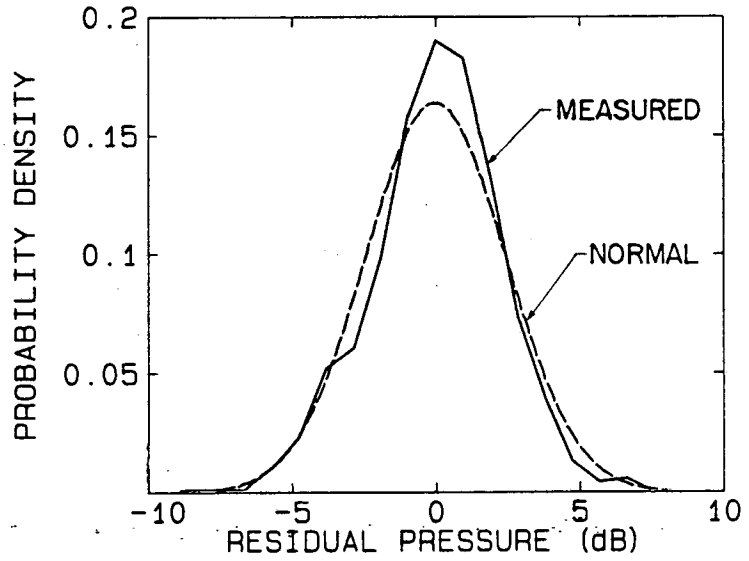

Figure 3: Composite residual probability distribution for single data sets. The normal probability distribution with zero mean and variance of 5.92 is also shown.

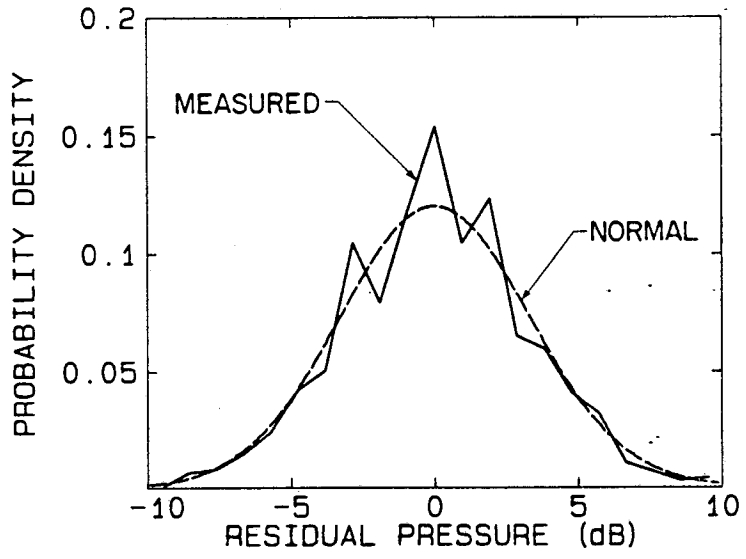

Figure 4: Composite residual probability distribution for combined data sets. The normal probability distribution with zero mean and variance of 10.99 is also shown.

Level %	Single Data Sets (dB)	Combined Data Sets (dB)
50	±1.63	±2.22
95	±4.77	±6.50
99	±6.25	±8.52

Table 3: Confidence intervals for noise measurements at various levels of confidence.

suggests that ship noise variability increases as the time between the measurements increases.

2.2.2 Correlation of Variability with Other Parameters

Another objective of this study was to examine statistically significant correlations between ship noise variability and other variables. The results of the previous section provide a framework for this.

As part of tests for adequacy of the regression model that were described at the end of Section 2.1.2, the residuals were plotted as functions of noise level, propeller rotation rate, and frequency. Visual examination of the scatter of the residuals about zero would show correlations between the variability and these variables, but no consistent trends were found between the noise variability and any of these variables.

3 Noise Transmission and Measurement

A number of phenomena can influence ship noise measurements. They affect either the characteristics of

1. the acoustic source,
2. the medium through which the acoustic waves propagate, or
3. the measurement system.

The reason for measuring ship noise is to determine the characteristics of the ship as an acoustic source. Thus, effects in the first of these categories should be separated from those in the latter two. Unfortunately, ship noise measurements must be done at sea where it is seldom possible to control or measure the experimental conditions sufficiently well so that full separation is possible.

In this section, this problem is considered by examining a conceptual model of the procedure commonly used to measure the radiated sound from ships. The purpose of this analysis is to provide realistic estimates of the errors inherent in a modern implementation of the technique.

Figure 5 schematically shows the model. The ship is assumed to move in a straight line at constant speed u past an omni-directional measuring hydrophone located at depth z_m. There is assumed to be a single compact acoustic source located on the moving ship at depth z_s. The horizontal distance from the hydrophone to the closest point of approach of the ship is y and the position along the ship track is x. The pressure at the hydrophone and ship position are

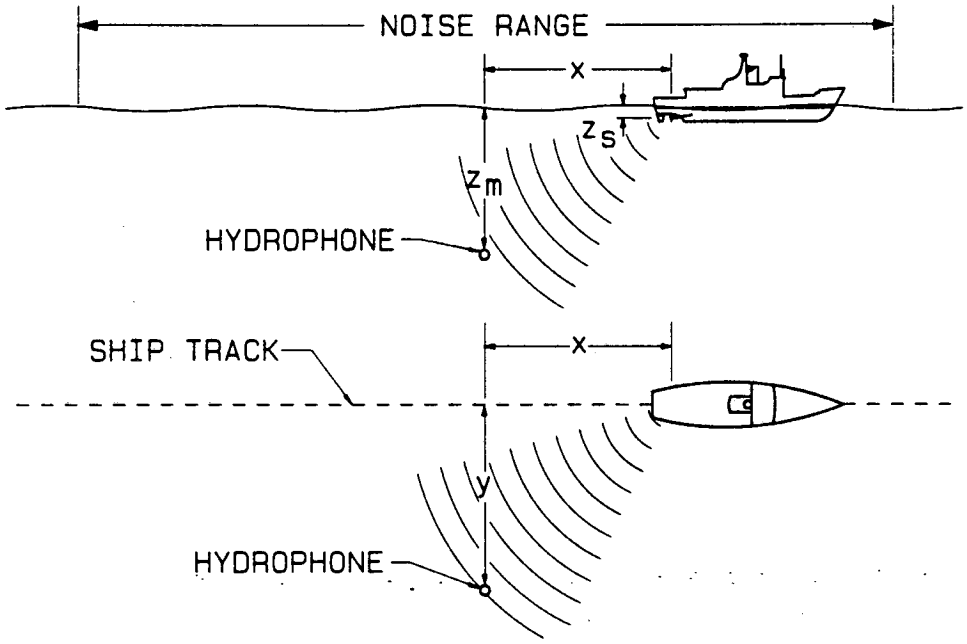

Figure 5: Ship noise measurement model

measured as functions of time. Then the power spectral density of the signal is computed by standard FFT techniques and averaged over the time T taken for the ship to pass over the noise range. All of the examples discussed below have y=100 m, z_s=5 m, z_m=10 m, and u=10 m/s.

Implicit in the use of conventional spectral analysis is the assumption that the measured signal is statistically stationary and ergodic, which basically means that the statistical properties do not change with time. If this is true, then the procedure for error analysis is well known. The problem here is that the signal received at the measurement hydrophone is not ergodic. This is due primarily to the motion of the acoustic source relative to the measurement hydrophone, and occurs even if the acoustic source itself might be considered ergodic if the measurements could be done in a stationary frame of reference. The following are important:

1. The effect of multiple sound transmission paths varies with the position of the ship.
2. The measured signal level changes as the distance from the ship to the hydrophone (range) changes.
3. Frequency information undergoes a Doppler shift which is a function of the speed of the ship relative to the measuring hydrophone.

The analysis below deals with these topics.

3.1 The Ideal Measurement

To unambiguously define the acoustic source characteristics, it is common to correct sound measurements to *free-field levels.* This term refers to the (fictitious) sound measurements that

would be made if the medium through which the sound propagates is both homogeneous and infinite in extent. Such a measurement would include only sound that travels in a straight line from the source to the receiver and not any effects due to reflection, refraction, or diffraction.

If, in addition, this ideal medium is lossless, then the acoustic pressure will always become asymptotically proportional to the distance from the source after a certain critical distance is exceeded. This type of pressure variation is called *spherical spreading* and the critical distance defines the edge of the *far-field.* Near the source, the acoustic pressure still may vary in a complicated way even in an ideal medium.

With these assumptions, if the acoustic pressure is known to be $P_s(t)$ at some reference distance r_0, then the acoustic pressure at any far-field point that is a distance r from the source is

$$P(r,t) = \frac{r_0}{r} P_s(t - r/c). \tag{14}$$

It is the idealized quantities P_s and its spectral density S_s which are to be estimated. Also, for reasons described later, the further condition is imposed that these quantities be measured in a frame of reference in which the source is stationary.

3.2 Measured Pressure

The pressure signal received at the measuring hydrophone is a combination of waves that travel by the direct path (quantities with subscript d) and those that travel by the surface reflected path (quantities with subscript r).

The length of the direct path is

$$r_d = \sqrt{x^2 + y^2 + (z_s - z_m)^2}. \tag{15}$$

Using the *method of images*, the length of the surface reflected path is

$$r_r = \sqrt{x^2 + y^2 + (z_s + z_m)^2}. \tag{16}$$

In these equations and those to follow, it is convenient to introduce the variables

$$a^2 = y^2 + (z_s - z_m)^2 \tag{17}$$

and

$$b^2 = y^2 + (z_s + z_m)^2. \tag{18}$$

The signal received at the hydrophone at time t is emitted from the source at an earlier time τ (called the *retarded time*) and propagates along the path at the speed of sound c. In this analysis $t = 0$ is assigned to the time of closest approach of the ship to the hydrophone with t negative as the ship approaches the hydrophone and positive after the ship passes. There is a different retarded time for each sound path. The retarded time for the direct path is

$$\tau_d = t - \frac{r_d}{c} = t - \frac{\sqrt{u^2\tau_d^2 + a^2}}{c} \tag{19}$$

and for the surface reflected path

$$\tau_r = t - \frac{r_r}{c} = t - \frac{\sqrt{u^2\tau_r^2 + b^2}}{c}. \tag{20}$$

Here use has been made of the fact that the x coordinate of the ship position at the time of emission of the sound is given by the ship speed u times the appropriate retarded time. Solving these equations for the retarded times in terms of t gives

$$\begin{aligned} \tau_d &= \frac{c^2 t - \sqrt{c^2 u^2 t^2 + a^2(c^2 - u^2)}}{(c^2 - u^2)} \\ \tau_r &= \frac{c^2 t - \sqrt{c^2 u^2 t^2 + b^2(c^2 - u^2)}}{(c^2 - u^2)}. \end{aligned} \tag{21}$$

The distances r_d, r_r, and the measured ship range r_m may be expressed in terms of t as

$$\begin{aligned} r_d &= \sqrt{u^2 \tau_d^2 + a^2} \\ r_r &= \sqrt{u^2 \tau_r^2 + b^2} \\ r_m &= \sqrt{u^2 t^2 + a^2}. \end{aligned} \tag{22}$$

Here r_m is the quantity that would be measured by an optical or micro-wave position tracking system. If an underwater acoustic range finder were used, r_m would probably equal r_d.

The measured acoustic pressure is

$$P_m(t) = P_n(t) + \frac{r_0}{r_d} P_s(\tau_d) + A_r \frac{r_0}{r_r} P_s(\tau_r). \tag{23}$$

This states that the measured pressure is the sum of waves that traveled by the direct path (second term, right side), waves that traveled by the surface reflected path (last term, right side), and the quantity $P_n(t)$ which includes all random noise components such as the ambient acoustic noise and electrical noise in the instrumentation. The quantity A_r is the reflection coefficient of the water surface. It has been assumed that pressure varies with path length according to the spherical spreading law. Thus, this model does not include any effects of refraction by non-uniform sound speed profiles.

A *range corrected* pressure $P_c(t)$ is then computed using the measured range, giving

$$P_c(t) = \frac{r_m}{r_0} P_m(t) = \frac{r_m}{r_0} \left(P_n(t) + \frac{r_0}{r_d} P_s(\tau_d) + A_r \frac{r_0}{r_r} P_s(\tau_r) \right). \tag{24}$$

3.3 Spectral Analysis

The purpose of the spectral analysis procedure is to calculate the *power spectral density* of $P_c(t)$. Currently, the most common technique for this is based on the Fast Fourier Transform (FFT) algorithm. (See Reference [4] for a detailed discussion of FFT analysis techniques.)

The power spectral density $S(f)$ of the function $P_c(t)$ is defined as

$$S(f) \equiv \lim_{T \to \infty} \frac{1}{T} \overline{\left| \int_{-T/2}^{T/2} P_c(t) e^{i\omega t} dt \right|^2}. \tag{25}$$

Here, T is the length of time taken for the measurement (called the measurement time). If $P_c(t)$ is ergodic, then the mean may be converted to a time average which is computed by dividing

the full measurement time into N blocks each of length T' and starting at T_j. The equation for the estimated power spectral density then becomes

$$S_e(f) = \frac{1}{NT'} \sum_{j=1}^{N} \left| \int_{T_j}^{T_j+T'} W(t) P_c(t) e^{i\omega t} dt \right|^2 . \tag{26}$$

The function $W(t)$ is a data window function which is introduced to suppress certain effects that result from the use of short data segments [4]. Numerous data windows with special properties have been used [5], but the most common one used for analysis of random data is the Hann window defined as

$$W(t) = \sqrt{\frac{8}{3}} \left[\frac{1 - \cos\left(\frac{2\pi(t-T_j)}{T'}\right)}{2} \right] . \tag{27}$$

It can be shown that the operation of sampling a signal for a finite length of time imposes a minimum frequency bandwidth, called the resolution bandwidth B_e, on the spectrum calculated by the above procedure. This means that no feature of the spectrum can appear to occupy a frequency band less than B_e in width. The resolution bandwidth is given approximately by

$$B_e = \frac{1}{T'} . \tag{28}$$

This effect tends to smooth out sharp features of the spectrum, and introduces a *bias error* into the estimated power spectral density. Reference [4] gives this as

$$\overline{S_e} \approx S + \frac{B_e^2}{24} \frac{\partial^2 S}{\partial f^2} . \tag{29}$$

To implement this spectral analysis procedure on a digital computer, the function $P_c(t)$ is first digitally sampled to produce a series of values of $P_c(t)$ at equal time intervals. This is called a *time series*. The integral in Equation 26 is efficiently computed from the time series using the FFT algorithm. The final power spectral density is found by averaging together a number of these raw spectral estimates.

To avoid a type of error called *aliasing*, the function $P_c(t)$ must not contain any components at frequencies greater than half the sample rate. In this case $P_c(t)$ is a measured signal, and so it must be filtered with an *analogue* low pass filter *before* it is digitally sampled. It will be assumed that this has been done.

Finally, S_e is only a random estimate of the power spectral density which hopefully improves in accuracy as more data is added to the average. For ergodic data, the variance of $S_e(f)$ is

$$\sigma^2_{S_e,r} = \frac{S^2}{N} . \tag{30}$$

Strictly, this is only true if $P_c(f)$ has a normal probability distribution, but Bendat and Piersol [4] argue that it is a good estimate no matter what the probability distribution as long as the resolution bandwidth is small.

3.4 Errors in Measured Quantities

Two measured quantities, r_m and P_m, are used in Equation 26 to calculate S_e. Each of these include uncertainty which has not been included in the analysis of the previous section.

A rigorous analysis of this error is complicated because of the complexity of Equation 26, but S is of the order

$$r_m^2 P_m^2. \tag{31}$$

Using the method of [6], the variance of S_e due to errors in r_m and P_m is

$$\sigma_{S_e,m}^2 \approx \left(\frac{\partial S}{\partial r_m}\sigma_{r_m}\right)^2 + \left(\frac{\partial S}{\partial P_m}\sigma_{P_m}\right)^2, \tag{32}$$

where σ_{r_m} and σ_{P_m} are the variances of r_m and P_m. This gives

$$\sigma_{S_e,m}^2 \approx \left(\frac{2\sigma_{r_m}}{r_m}\right)^2 S^2 + \left(\frac{2\sigma_{P_m}}{P_m}\right)^2 S^2. \tag{33}$$

Equations 30 and 33 describe different components of the random error in S_e, but are not sufficient to explain the variance found in the statistical analysis.

3.5 Doppler Shift

The frequency of the measured sound differs from the source frequency if the source is in motion relative to the receiver. This is called a Doppler shift. The instantaneous measured frequency is

$$f_m = \frac{f_s}{1 - (u/c)\cos\theta} \tag{34}$$

where θ is the angle between the ship velocity vector and the direction of the sound path at the source position (see Figure 6). The measured frequency is higher that the emitted sound frequency as the ship approaches the receiver, equal at the closest point of approach, and lower after the ship has passed.

The spectral analysis procedure includes an average over the measurement time, and so the Doppler shift is also averaged over this time. Figure 7 shows the results for a 1000 Hz source line with measurement times of 25 and 100 seconds. The line appears spread out. With very long measurement times, θ varies almost from 0 to π, giving a maximum spread of 14 Hz for a ship speed of 10 m/s. At shorter times the spread is less.

3.6 Multi-Path Transmission

Since S_s is estimated from ship noise measurements which must be made at sea, it is important to examine how the ocean differs from a true free-field environment and determine how this affects the results.

Sound is refracted in the ocean due to variations in water temperature, pressure, and salinity. In some circumstances this may affect ship noise measurements, but here it is assumed that the distance from acoustic source to the measurement hydrophone is small enough that refractive effects can be ignored. If the distance is less than one kilometer, this should be a good assumption.

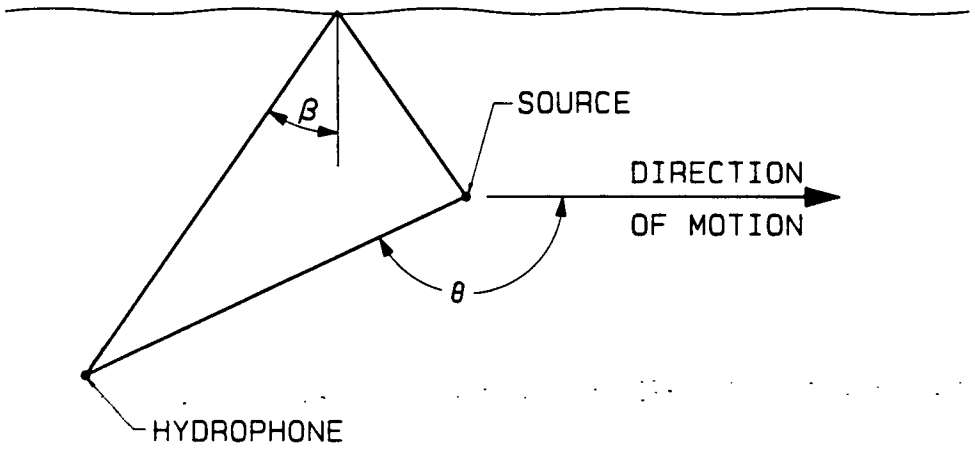

Figure 6: Sound path geometry

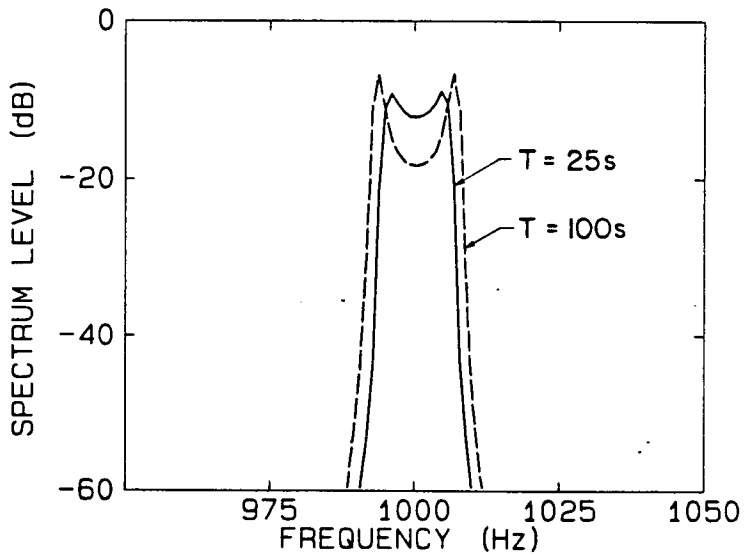

Figure 7: Effect of Doppler shift on a 1000 Hz source line for measurement times of 25 and 100 seconds

The reflection of sound does affect ship noise measurements significantly. The air-water surface is a good reflector of sound, and so surface reflections are usually important and are treated in the following discussion. Reflections from the sea bottom may also be important, but are more difficult to treat. Also, if the measurements are carried out in deep water or over areas of sea-bed with high acoustic absorption, reflections from the sea bottom may be negligible. Thus, bottom reflections are not treated in detail, but their effects should be qualitatively similar to those of the surface reflections.

Figure 6 shows the geometry of the sound paths. Sound that travels by the surface reflected path takes slightly longer to reach the hydrophone than the direct path sound. The resulting phase difference causes an interference effect sometimes called the *Lloyd's mirror* effect.

As shown in Appendix B, if the source and receiver are both stationary, the power spectral density of the measured sound $S_r(f)$ is related to $S_s(f)$ by

$$S_r(f) = \left[1 + 2A_r\frac{r_d}{r_r}\cos\omega(\tau_d - \tau_r) + A_r^2\frac{r_d^2}{r_r^2}\right] S_s(f). \tag{35}$$

Here the acoustic source is moving, but the spectral analysis procedure treats the time series in short segments over which the difference in time delays is nearly constant. Thus, the measured power spectral density S_m is approximately the average of S_r over the total measurement time, and so

$$\frac{S_m(f)}{S_s(f)} = \frac{1}{T}\int_{-T/2}^{T/2}\left[1 + 2A_r\frac{r_d}{r_r}\cos\omega(\tau_d - \tau_r) + A_r^2\frac{r_d^2}{r_r^2}\right] dt. \tag{36}$$

The quantity A_r is the reflection coefficient. For a flat water surface it has a value very close to minus one for all angles of incidence, but for rough surfaces A_r becomes a function of angle of incidence and frequency. As shown in Reference [7], a good approximation is

$$A_r = -\exp\left[-2\left(\frac{\omega\sigma_s\cos\beta}{c}\right)^2\right]. \tag{37}$$

Here, σ_s is the root mean squared surface roughness and β is the angle of incidence (see Figure 6). The value of σ_s is approximately the significant wave height divided by four. The significant wave height can be found from sea state tables [8]. Sea state zero would correspond to a σ_s of zero, for sea state one the maximum σ_s is approximately 0.025 m, and for sea state two it is 0.125 m.

Equation 36 gives the error in the measured power spectral density that is induced by the effect of the surface reflection. The integral was evaluated numerically and the results for a flat sea surface (reflection coefficient of minus one) and no attenuation are shown in Figure 8 as a function of frequency for several measurement times. At low frequencies the error is a strong function of frequency and the length of time taken for the measurement. While at high frequencies the error gradually steadies down to nearly 3 dB.

This error is also a function of sea state. Figures 9 and 10 compare the error due to surface reflections for a flat sea to that with a σ_s of 0.125 m (top of sea state 2). Figure 9 was calculated with a measurement time of 25 seconds and Figure 10 with 100 seconds. In both cases the rough sea surface reduces the high frequency reflection coefficient so that error due to surface reflections is virtually eliminated at 50 kHz. The results with the longer measurement time show

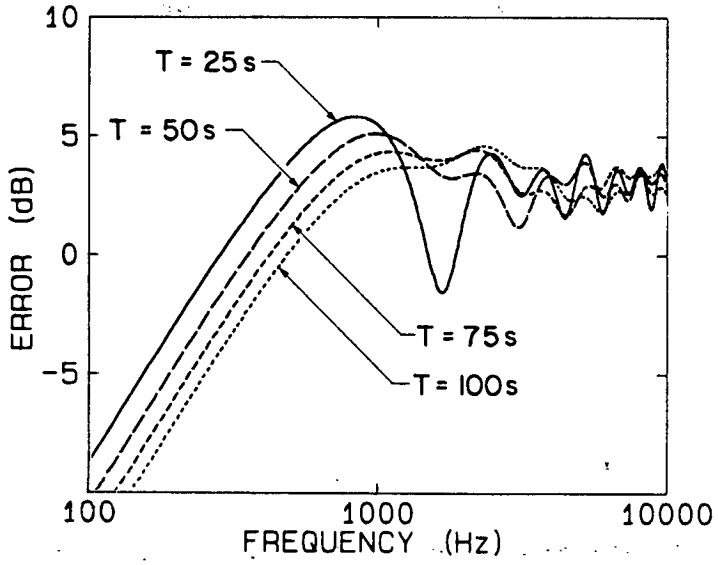

Figure 8: Lloyd's mirror correction vs. frequency for measurement times of 25, 50, 75, and 100 seconds

more error at high frequencies because more data is included in the average from times when the source is far away and β is large (resulting in a large reflection coefficient).

These results were calculated without attenuation, but its inclusion would not greatly affect this component of error because the attenuation is nearly equal for the two paths. Also, Equation 36 cannot describe a Doppler shift. This would be important at high frequencies where it would smooth out the ripples in the spectrum.

3.7 Attenuation

Another important factor in the measurement of source strength is the attenuation that occurs as the sound propagates along its path. The pressure varies as

$$P = P_s \exp(-\alpha_e r). \tag{38}$$

Here α_e is the attenuation coefficient. It is more common to express this in terms of the logarithmic attenuation coefficient α which is found from

$$\frac{1}{r} 20 \log\left(\frac{P_s}{P}\right) = 8.686\alpha_e = \alpha, \tag{39}$$

where α is expressed in units of dB loss per unit distance.

Near the ocean surface there are two important components of this attenuation: the attenuation of pure sea water, and that due to suspended bubbles.

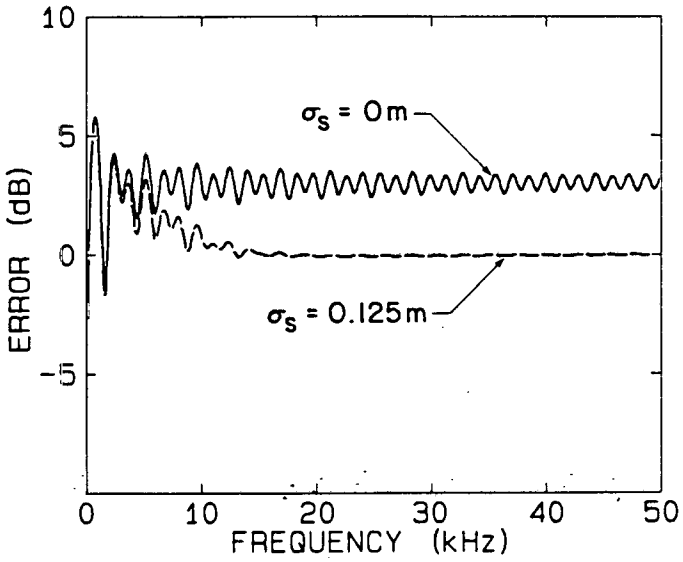

Figure 9: Lloyd's mirror correction vs. frequency for rms sea roughnesses of 0 and 0.125 m, measurement time is 25 seconds

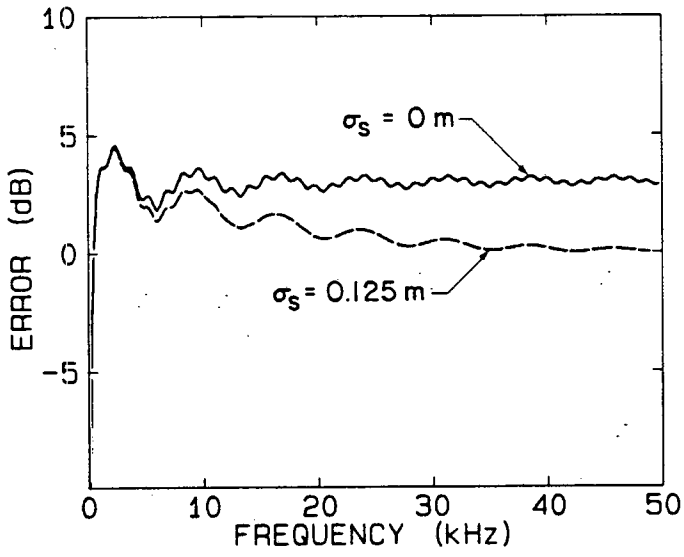

Figure 10: Lloyd's mirror correction vs. frequency for rms sea roughnesses of 0 and 0.125 m, measurement time is 100 seconds

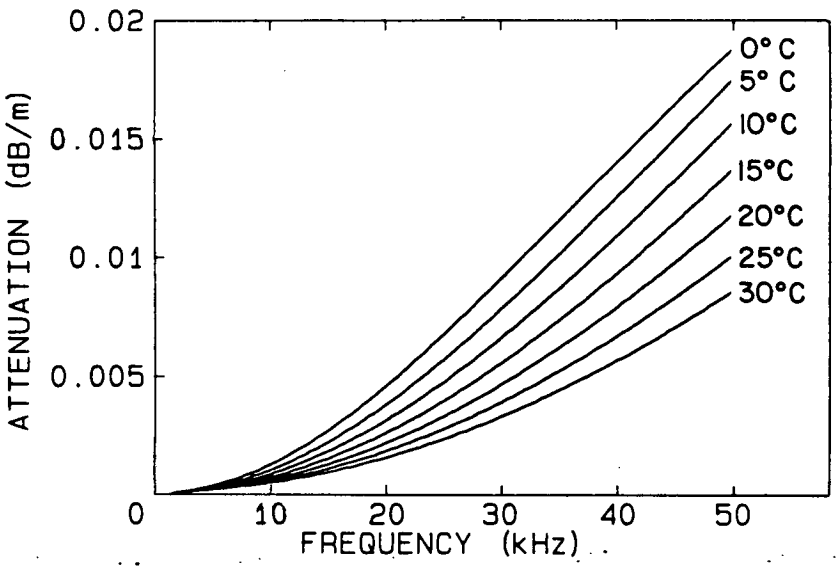

Figure 11: Attenuation coefficient vs. frequency for various water temperatures (salinity of 35 parts per thousand)

3.7.1 Pure Sea Water

The attenuation of pure sea water is a function of frequency, temperature and salinity. The variation with frequency at various temperatures is shown in Figure 11, as calculated by the method in Reference [7] for a salinity of 35 parts per thousand by weight. The attenuation of pure sea water is very small below 5 kHz, increases roughly as f^2 to nearly 100 kHz, and decreases with increased temperature.

The results of including this attenuation in the error calculation of Equation 36 are shown in Figures 12 and 13. Figure 12 shows the results for calm water, temperatures of 5 and 20 C, and a 25 second measurement time. The attenuation is greatest at high frequency and the difference in temperature causes approximately 0.8 dB difference in error at 50 kHz. The longer measurement time, shown in Figure 13, causes the effect to be more pronounced because the average then includes sound that travels over longer paths.

3.7.2 Suspended Bubbles

The sound attenuation just described applies deep in the ocean. Near the surface the water may contain small quantities air bubbles which greatly increase the attenuation over that of pure sea water.

A number of measurements of the number and size of bubbles in sea water are reviewed in Reference [9]. Near the water surface the action of wind and waves cause small air bubbles to be mixed into the water column. The large bubbles rapidly rise to the surface leaving a distribution of smaller bubbles which rise less quickly. In deep water far from land this is the

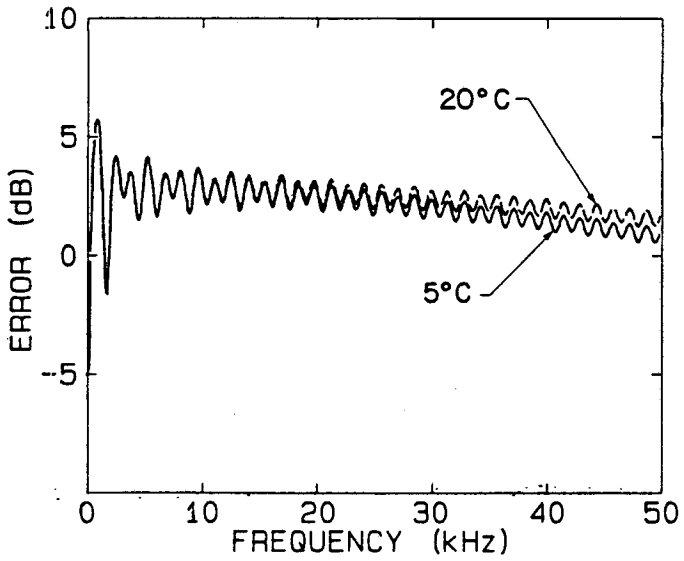

Figure 12: Lloyd's mirror correction vs. frequency for water temperatures of 5 and 20 C, measurement time is 25 seconds

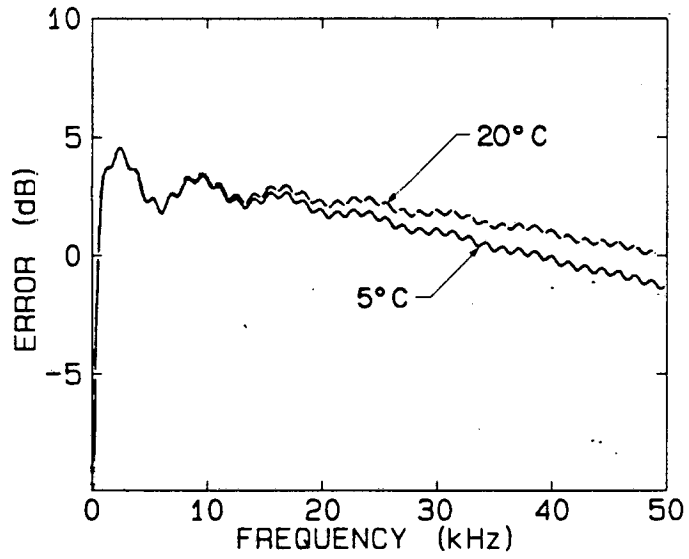

Figure 13: Lloyd's mirror correction vs. frequency for water temperatures of 5 and 20 C, measurement time is 100 seconds

dominant method of bubble formation and the number of bubbles per unit volume (bubble density) varies exponentially with water depth and is a function of wind speed. In shallow water near land the bubble density does not diminish as quickly with depth nor is it as strong a function of wind speed, suggesting other sources of bubbles such as: wave activity against the coast, biological activity, or bubbles carried into the sea from rivers.

The motion of a surface ship also adds bubbles to the water. The wake behind the ship is an area of turbulent water containing many bubbles which may persist for hours after passage of the ship. Also, the rolling motion of the ship may trap air under portions of the hull such as the bilge keels. Thus, a surface ship which repeatedly passes through the same area of water may increase the bubble density in that area.

The attenuation caused by these bubbles is very dependent on both the sound frequency and the bubble sizes. Laboratory measurements with water containing bubbles all of nearly equal size show that the attenuation near the resonance frequency of the bubbles is over 100 dB per meter for air contents as low as 0.05 percent by volume, but drops off quickly at frequencies away from resonance [10,11]. Sea water, on the other hand, will contain bubbles of many sizes which resonate at different frequencies, and so will have a relatively broad peak in the attenuation curve.

The attenuation that is actually measured in any particular circumstance cannot be predicted unless the distribution of bubble sizes along the path the sound takes from the source to the measurement point is known. Novarini and Bruno [12] attempted such a calculation. They derived an empirical formula for the bubble size distribution for the deep ocean as a function of water depth and wind speed, which they used to study refraction and attenuation of sound by the surface bubble layer. They showed the bubbles could form a sound channel at the surface and estimated the attenuation per limiting ray cycle (approximately 4 km) of 10 kHz sound trapped in this layer as nearly 6 dB for 15 knot winds and between 35 to 40 dB for 25 knot winds. The attenuation of sound that leaves the bubble layer was found to be strong function of the source and receiver position in the layer.

These results show such a strong dependence on the sound path and bubble size distribution that practical calculations are very difficult. Still, there is good reason to believe that surface bubbles significantly affect ship noise measurements if either the acoustic source or the hydrophone are within the bubble layer. The amount of attenuation may vary significantly over a short period of time (several hours) in response to changes in the bubble distribution brought about by changing wind conditions or the build up of bubbles introduced by the ship wake.

3.8 Combined Errors

So far each type of error has been considered separately, but in reality they are all combined. Figure 14 compares the combined errors due to surface reflections and pure sea water attenuation for two different (but reasonable) situations. One case is for a flat sea, 20 C water temperature, and a 25 second measurement time. The other is for sea state 2, 5 C water temperature, and a 100 second measurement time. The ship noise spectra measured under these conditions would differ by as much as 7 dB at some frequencies. The effect of suspended bubbles was not included here, but would lead to even greater variability.

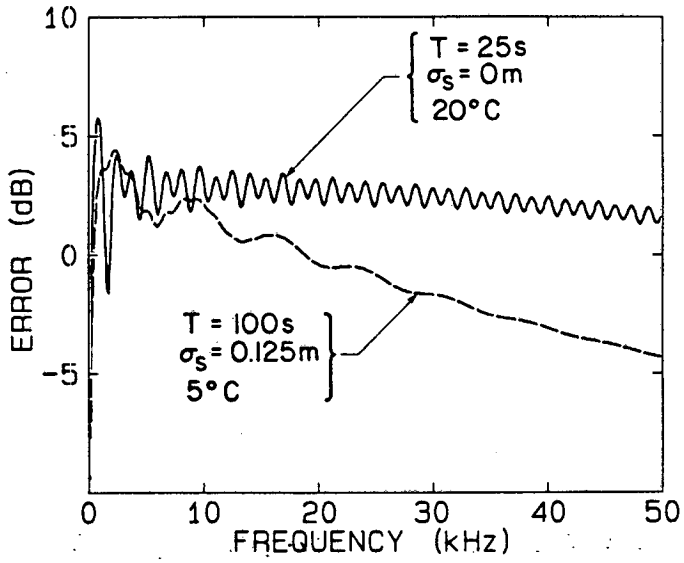

Figure 14: Error calculated for two specific cases

3.9 Choice of Measurement Time

Previous discussions have shown that the measurement time is an important parameter, but did not indicate how to choose it.

The most basic consideration is that the measurement time be long enough so that the uncertainty of the spectral density (given by Equations 9 and 30) meets the desired limit. Also, if the ship is rolling, the noise measurement should extend over several roll periods (each on the order of 10 seconds). If this amount of data cannot be obtained in a single pass by the hydrophone, then spectra from additional passes should be averaged until the total measurement time meets the requirement.

All of the examples of errors due to surface reflections and attenuation were calculated with a ship speed of 10 m/s. At other speeds, the same error curves apply as long as the geometry of the sound paths is the same. This requires that the noise be measured over a constant portion of the ship's track past the hydrophone. (In other words the noise should be averaged over a constant range of x coordinates.) This requires the measurement time to vary inversely with ship speed.

4 Propeller Cavitation

So far effects related to the transmission and measurement of sound have been examined, but not variation of the actual acoustic source level. This section deals with factors which affect propeller cavitation as a noise source.

The cavitation can change in two ways. First, the ship speed at which it first occurs (called the inception speed) may change. Second, at speeds above inception, new types of cavitation

may form or the relative quantity of each of the types may vary.

These changes in the cavitation can be produced in several ways.

1. If the propeller is controllable pitch, the pitch must be accurately set, which may be difficult to do accurately.

2. Any damage to the propeller or fouling (perhaps by marine growth, rope or fishing nets) would greatly increase the cavitation.

3. A change in the depth of the propeller (for example caused by a change in ship draught) alters the cavitation inception speeds.

4. A change in the propeller inflow velocity distribution will vary both the types of cavitation and the inception speeds. This could be caused by modifications to the hull especially the addition of appendages, by cross flow introduced by ship motions or water current, or by rudder action required to maintain course.

5. An increase in the ship resistance will cause more cavitation due to the increased loading of the propeller.

If the geometry of the ship and propeller are constant, then the last two of these factors are most important. Of these, it is possible to quantify the effect of ship resistance on cavitation.

4.1 Ship Resistance

As discussed above, the ship resistance is an important factor in determining the amount of propeller cavitation and thereby the noise level. To illustrate this, an estimate of the change in noise due to a 10 percent increase in ship resistance is presented.

Suppose that back sheet cavitation is the dominant form of cavitation. The discussion in Reference [13] (Section 16.7 of Chapter VII) suggests that a 10 percent increase in ship resistance would increase the inception cavitation number by 20 percent. The slope of the noise level versus cavitation number curve is required to estimate the resulting increase in noise. Reference [14] includes such a curve for hydrofoil surface cavitation, which shows that an increase in inception cavitation number of this size could cause an increase in the sound levels of over 10 dB.

This calculation should be considered as only a rough estimate. Better results could be achieved by considering model test results for particular ships, but the conclusion would still be that changes in ship resistance of the order considered here can significantly affect the noise output from propeller cavitation. Several factors that affect the ship resistance will now be discussed.

4.1.1 Shallow Water

In very deep water, ship performance is independent of the actual depth. This is not true in shallow water. The nearby ocean bottom alters both the surface wave pattern produced by the ship and the velocity of the water beneath the hull. This causes the draught, trim, and ship resistance to change from the values in deep water.

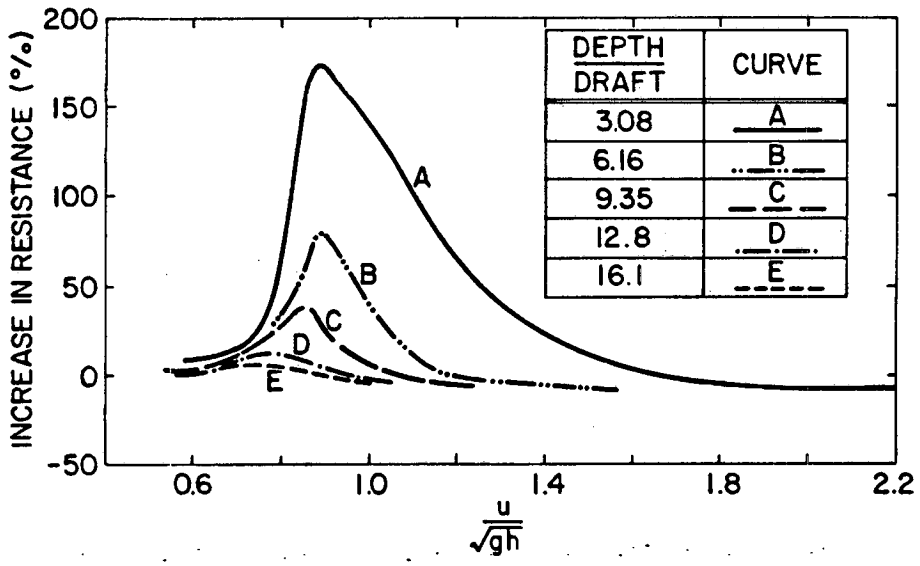

Figure 15: Percentage increase in ship resistance in shallow water (figure reprinted from Reference [13])

Detailed methods of estimating the change in ship resistance in shallow water are given in Reference [13] and Figure 15 illustrates a specific example. A critical parameter is the dimensionless quantity

$$F_n = \frac{u}{\sqrt{gh}}, \tag{40}$$

where u is the ship speed, g is the acceleration due to gravity, and h is the water depth. The effect of water depth is negligible if this quantity is less than 0.4. The ship resistance reaches a maximum at values of F_n between 0.8 and 1.

As an example, suppose that a ship with 5 metre draught is in 30 metres of water. Curve B of Figure 15 suggests that the ship resistance exceeds the deep water value by 10 percent when F_n is greater than 0.7, which corresponds to a ship speed of 12 m/s (23 knots).

4.1.2 Other Effects

During the normal operation of a ship the draught and trim may change due to consumption of fuel or addition of equipment and cargo. These change the wetted surface area and possibly the surface wave pattern, which will affect the ship resistance.

The resistance also depends upon the condition of the hull surface. A ship is usually smoothest and has the lowest resistance immediately after the hull is painted and increases after that. For conventional paints the increase in resistance may be from 20 to 30 percent in the first year of operation [13]. For newer self-polishing anti-fouling paints this is not such a problem.

4.2 Environmental Factors

It is best to measure ship noise in flat seas with no wind or water current. Unfortunately, these ideal conditions are seldom available. The following discussion considers how poorer conditions affect ship noise.

Water current does not affect ship performance other than to change the velocity vector. A current directed along or opposite the ship heading alters the speed over the ground, but not the radiated noise. On the other hand, a cross current may cause greater propeller cavitation if significant rudder must be applied to keep the ship on the required course.

Compared to this, wind usually has a much larger effect. The force applied to the ship is proportional to the squared magnitude of the apparent wind (wind measured relative to the ship velocity vector) and varies with direction. For a ship moving directly upwind or downwind, this force changes mainly the ship resistance. Reference [13] suggests that an apparent head wind of 15 m/s will increase resistance from 5 to 20 percent (depending on the superstructure) over that with zero apparent wind. Wind that is not directly on the bow or stern will cause the ship to list and yaw, as well as require significant rudder to maintain course.

Finally, a rough sea influences all aspects of ship performance and greatly increases propeller cavitation. The ship resistance increases, as do all of the components of ship motion (such as roll, pitch, etc.). These effects cause the propeller loading to vary as the ship moves in the sea, which causes the amount of cavitation to vary. Also, air can be trapped under parts of the hull, such as bilge keels, and be swept into the propeller causing great changes in the noise produced by the cavitation.

5 Conclusions

This paper examined the variability of far-field noise from ship propeller cavitation. An analysis of some naval ship data provided statistical information about the variability, but revealed little about its causes. Further discussion of phenomena that affect ship noise measurements showed that the statistical results were reasonable and identified a number of areas where ship noise measurement practice could be improved.

The normal probability density function adequately described the variability of the noise spectra considered here. The variability did not depend upon noise level, frequency, or propeller revolution rate, but the time between measurements was important. Data sets measured over a period of years had greater variability than sets containing data taken over a few days.

The confidence intervals in Table 3 are based on these results. They are valid when broadband cavitation noise is the dominant noise source, for frequencies above the spectral peak. These confidence intervals provide a good indication of the variability, but are based only on data for three ships measured at one noise range. More general results would require data from more ships and noise ranges.

Part of the variability is due to random error in the spectral analysis procedure, and uncertainty in the measurements of sound pressure and distance from the ship to the hydrophone. These are an inherent part of any noise measurement and are well understood. Unfortunately, they are insufficient to explain the variability of ship noise data.

The sound transmission properties of the ocean cause part of the additional variability. Sea roughness affects the amount of high frequency sound reflected from the ocean surface. Water

temperature and salinity, as well as the number of suspended gas bubbles, affect the attenuation of sound. These phenomena can cause ship noise measurements to vary by more than 5 dB, sufficient to explain the statistical results. This could happen over a period of several hours. Thus, sound transmission measurements would be required several times a day to monitor these effects.

The geometry of the sound paths, which is determined by the positions of the ship and hydrophone, also affects the transmission properties. This source of variability can be minimized by always measuring the noise over a constant portion of the ship's track past the hydrophone.

Finally, the noise produced by the cavitation may vary. This may result from changes in ship resistance due to operation of the ship in shallow water, as well as changes in hull roughness, draught, and trim. Also, deviation from the ideal environmental conditions of flat seas with no wind or water current will cause greater noise.

6 Recommendations for Ship Noise Measurement

The following recommendations will help control the variability of ship noise measurements and should be implemented:

1. Noise ranges should calculate confidence intervals for their measurements, possibly using the procedure described in Section 2.1.2. The distinction between short term and long term variability is important and separate confidence intervals should be determined for each.

2. The sound transmission properties of the water should be measured using broadband acoustic sources located at several positions along the ship track and at the same depth as the ship's dominant noise source. This should be done several times a day especially if the weather changes.

3. The test program should be done in random order to prevent changes in sound transmission properties from introducing systematic errors.

4. The noise should be measured over a constant portion of the ship's track past the hydrophone.

5. In all but flat seas, the noise measurement should include data from several ship roll periods (each around 10 seconds).

6. Both shaft power and revolution rate should be measured to indicate changes in ship resistance.

7. Environmental conditions such as sea state, wind, and water temperature should be recorded.

8. The maximum ship speed should be less than $0.4\sqrt{gh}$. At speeds above this limit, ship resistance depends strongly on water depth, causing the cavitation noise to be different from that in deep water.

9. Water currents which cause the ship to apply significant rudder to maintain course should be avoided. On the other hand, currents along or opposite the ship heading do not affect noise. Currents in any direction sweep away air bubbles introduced into the sound range area by the ship's motion.

Appendix A

Given a set of m data points of the form (x_i, y_i, z_i), a solution is sought for the regression coefficients b_i in the regression model

$$z = b_0 + b_1 x + b_2 x^2 + b_3 x^3 + b_4 y + b_5 y^2 + b_6 y^3 + b_7 xy + b_8 x^2 y + b_9 x y^2. \tag{A.1}$$

The regression coefficients are found, as shown in Reference [2], from the solution of the matrix equation

$$\mathbf{AB} = \mathbf{C}. \tag{A.2}$$

For the stated regression model

$$\mathbf{A} = \sum_{i=1}^{m} \begin{bmatrix} 1 & x_i & x_i^2 & x_i^3 & y_i & y_i^2 & y_i^3 & x_i y_i & x_i^2 y_i & x_i y_i^2 \\ & x_i^2 & x_i^3 & x_i^4 & x_i y_i & x_i y_i^2 & x_i y_i^3 & x_i^2 y_i & x_i^3 y_i & x_i^2 y_i^2 \\ & & x_i^4 & x_i^5 & x_i^2 y_i & x_i^2 y_i^2 & x_i^2 y_i^3 & x_i^3 y_i & x_i^4 y_i & x_i^3 y_i^2 \\ & & & x_i^6 & x_i^3 y_i & x_i^3 y_i^2 & x_i^3 y_i^3 & x_i^4 y_i & x_i^5 y_i & x_i^4 y_i^2 \\ & & & & y_i^2 & y_i^3 & y_i^4 & x_i y_i^2 & x_i^2 y_i^2 & x_i y_i^3 \\ & & & & & y_i^4 & y_i^5 & x_i y_i^3 & x_i^2 y_i^3 & x_i y_i^4 \\ & & & & & & y_i^6 & x_i y_i^4 & x_i^2 y_i^4 & x_i y_i^5 \\ & & & & & & & x_i^2 y_i^2 & x_i^3 y_i^2 & x_i^2 y_i^3 \\ & & & & & & & & x_i^4 y_i^2 & x_i^3 y_i^3 \\ & & & & & & & & & x_i^2 y_i^4 \end{bmatrix}, \tag{A.3}$$

$$\mathbf{B} = \begin{bmatrix} b_0 \\ b_1 \\ b_2 \\ b_3 \\ b_4 \\ b_5 \\ b_6 \\ b_7 \\ b_8 \\ b_9 \end{bmatrix}, \tag{A.4}$$

and

$$\mathbf{C} = \sum_{i=1}^{m} \begin{bmatrix} z_i \\ x_i z_i \\ x_i^2 z_i \\ x_i^3 z_i \\ y_i z_i \\ y_i^2 z_i \\ y_i^3 z_i \\ x_i y_i z_i \\ x_i^2 y_i z_i \\ x_i y_i^2 z_i \end{bmatrix}. \tag{A.5}$$

The solution procedure consisted of first constructing the matrices $\mathbf{A}$ and $\mathbf{C}$ from the m data points, and then determining the matrix of regression coefficients, $\mathbf{B}$, using a numerical subroutine for solution of simultaneous linear equations.

The coefficient of multiple determination is

$$R^2 = \frac{m\mathbf{B}^T\mathbf{C} - (\sum z_i)^2}{m\sum z_i^2 - (\sum z_i)^2} \tag{A.6}$$

where $\mathbf{B}^T$ is the transpose of matrix $\mathbf{B}$.

Appendix B

In this appendix, the power spectral density of a signal that contains a reflection is calculated. The signal is assumed to be of the form

$$f(t) = f_0(t) + Af_0(t - t_0), \tag{B.1}$$

where $f_0(t)$ is the unreflected signal, A is the strength of the reflected signal, and t_0 is the amount the reflected signal is delayed.

The Fourier transform of this is

$$F(\omega) = \int_{-\infty}^{\infty} f_0(t)e^{i\omega t}dt + A\int_{-\infty}^{\infty} f_0(t - t_0)e^{i\omega t}dt. \tag{B.2}$$

Changing variables to $t' = t - t_0$ in the second integral gives

$$F(\omega) = \int_{-\infty}^{\infty} f_0(t)e^{i\omega t}dt + Ae^{i\omega t_0}\int_{-\infty}^{\infty} f_0(t')e^{i\omega t'}dt'. \tag{B.3}$$

Both of these integrals are the Fourier transform of $f_0(t)$, and so

$$F(\omega) = \left(1 + Ae^{i\omega t_0}\right) F_0(\omega). \tag{B.4}$$

The power spectral density is proportional to $|F(\omega)|^2$ which is

$$\begin{aligned} |F(\omega)|^2 &= F(\omega)F^*(\omega) \\ &= \left(1 + Ae^{i\omega t_0}\right)\left(1 + Ae^{-i\omega t_0}\right)|F_0(\omega)|^2 \\ &= \left[1 + A\left(e^{i\omega t_0} + e^{-i\omega t_0}\right) + A^2\right]|F_0(\omega)|^2. \end{aligned} \tag{B.5}$$

Now, Euler's Formula can be used to replace the exponentials with $2\cos(\omega t_0)$ giving

$$|F(\omega)|^2 = \left[1 + 2A\cos(\omega t_0) + A^2\right]|F_0(\omega)|^2. \tag{B.6}$$

References

[1] R. E. Walpole and R. H. Myers. *Probability and Statistics for Engineers and Scientists.* Macmillan Publishing Company, 1972.

[2] N. R. Draper and H. Smith. *Applied Regression Analysis.* John Wiley and Sons, 1966.

[3] D. Ross. *Mechanics of Underwater Noise.* Pergamon Press, 1976.

[4] J. S. Bendat and A. G. Piersol. *Random Data: Analysis and Measurement Procedures.* John Wiley and Sons, second edition, 1986.

[5] F. J. Harris. On the use of windows for harmonic analysis with the discrete fourier transform. *Proceedings of the IEEE*, 66:51–83, 1978.

[6] R. B. Abernethy, R. P. Benedict, and R. B. Dowdell. ASME measurement uncertainty. *Journal of Fluids Engineering*, 107:161–164, June 1985.

[7] C. S. Clay and H. Medwin. *Acoustical Oceanography: Principles and Applications.* John Wiley and Sons, 1977.

[8] S. L. Bales. Designing ships to the natural environment. In *19th Annual Technical Symposium, Association of Scientists and Engineers of the Naval Sea Systems Command*, 1982.

[9] J. Wu. Bubble populations and spectra in near-surface ocean: summary and review of field measurements. *Journal of Geophysical Research*, 86:457–463, January 1981.

[10] F. E. Fox, R. C. Stanley, and G. S Larson. Phase velocity and absorption measurements in water containing air bubbles. *Journal of the Acoustical Society of America*, 27:534–539, May 1955.

[11] E. Silberman. Sound velocity and attenuation in bubbly mixtures measured in standing wave tubes. *Journal of the Acoustical Society of America*, 29:925–933, August 1957.

[12] J. C. Novarini and D. R. Bruno. Effects of the sub-surface bubble layer on sound propagation. *Journal of the Acoustical Society of America*, 72:510–514, August 1982.

[13] J. P. Comstock, editor. *Principles of Naval Architecture.* The Society of Naval Architects and Marine Engineers, 1977.

[14] W. K. Blake, M. J. Wolpert, and F. E. Geib. Cavitation noise and inception as influenced by boundary-layer development on a hydrofoil. *Journal of Fluid Mechanics*, 80:617–640, 1977.

DOCUMENT CONTROL DATA

(Security classification of title, body of abstract and indexing annotation must be entered when the overall document is classified)

1. ORIGINATOR (the name and address of the organization preparing the document. Organizations for whom the document was prepared, e.g. Establishment sponsoring a contractor's report, or tasking agency, are entered in section 8.)

Defence Research Establishment Atlantic

2. SECURITY CLASSIFICATION (overall security classification of the document. including special warning terms if applicable)

Unclassified

3. TITLE (the complete document title as indicated on the title page. Its classification should be indicated by the appropriate abbreviation (S,C,R or U) in parentheses after the title.)

Variability of Ship Noise Measurements

4. AUTHORS (Last name, first name, middle initial. If military, show rank, e.g. Doe, Maj. John E.)

Sponagle, Neil C.

5. DATE OF PUBLICATION (month and year of publication of document)

June 1988

6a. NO. OF PAGES (total containing information. Include Annexes, Appendices, etc.)

38

6b. NO. OF REFS (total cited in document)

14

6. DESCRIPTIVE NOTES (the category of the document, e.g. technical report, technical note or memorandum. If appropriate, enter the type of report, e.g. interim, progress, summary, annual or final. Give the inclusive dates when a specific reporting period is covered.)

DREA Technical Memorandum

8. SPONSORING ACTIVITY (the name of the department project office or laboratory sponsoring the research and development. Include the address.)

Defence Research Establishment Atlantic
PO Box 1012, Dartmouth, N.S. Canada B2Y 3Z7

9a. PROJECT OR GRANT NO. (if appropriate, the applicable research and development project or grant number under which the document was written. Please specify whether project or grant)

9b. CONTRACT NO. (if appropriate, the applicable number under which the document was written)

10a. ORIGINATOR'S DOCUMENT NUMBER (the official document number by which the document is identified by the originating activity. This number must be unique to this document.)

DREA TECH MEMORANDUM 88/210.

10b. OTHER DOCUMENT NOS. (Any other numbers which may be assigned this document either by the originator or by the sponsor)

11. DOCUMENT AVAILABILITY (any limitations on further dissemination of the document, other than those imposed by security classification)

(X) Unlimited distribution
( ) Distribution limited to defence departments and defence contractors; further distribution only as approved
( ) Distribution limited to defence departments and Canadian defence contractors; further distribution only as approved
( ) Distribution limited to government departments and agencies; further distribution only as approved
( ) Distribution limited to defence departments; further distribution only as approved
( ) Other (please specify):

12. DOCUMENT ANNOUNCEMENT (any limitation to the bibliographic announcement of this document. This will normally correspond to the Document Availability (11). However, where further distribution (beyond the audience specified in 11) is possible, a wider announcement audience may be selected.)

13. ABSTRACT (a brief and factual summary of the document. It may also appear elsewhere in the body of the document itself. It is highly desirable that the abstract of classified documents be unclassified. Each paragraph of the abstract shall begin with an indication of the security classification of the information in the paragraph (unless the document itself is unclassified) represented as (S), (C), (R), or (U). It is not necessary to include here abstracts in both offical languages unless the text is bilingual).

S // Ship noise measurements are subject to relatively large variations that should be considered when these data are used. For modern naval ships operating at high speeds, propeller cavitation is the dominant source of radiated noise. This paper examines the variability of the broadband component of propeller cavitation noise based on statistical analysis of repeated measurements for several ships and propellers and on a conceptual model of the measurement process. Confidence intervals are determined for measured noise spectra and correlations are sought between the variability and certain important parameters. To explain these results, a number of phenomena are discussed that affect either the sound transmission properties of the water, the measurement procedure, or the acoustic source strength of propeller cavitation. //

14. KEYWORDS, DESCRIPTORS or IDENTIFIERS (technically meaningful terms or short phrases that characterize a document and could be helpful in cataloguing the document. They should be selected so that no security classification is required. Identifiers, such as equipment model designation, trade name, military project code name, geographic location may also be included. If possible keywords should be selected from a published thesaurus. e.g. Thesaurus of Engineering and Scientific Terms (TEST) and that thesaurus-identified. If it is not possible to select indexing terms which are Unclassified, the classification of each should be indicated as with the title.)

Ship Noise
Cavitation
Sound Ranges
Propeller
Variability

88-04312
#57517